Science Translational Medicine
AAAS

Epigenetic Reprogramming of *HOXC10* in Endocrine-Resistant Breast Cancer

Thushangi N. Pathiraja *et al.*

Sci Transl Med **6**, 229ra41 (2014);
DOI: 10.1126/scitranslmed.3008326

Editor's Summary

Playing Tug-of-War with *HOXC10*

Aromatase inhibitors are drugs that prevent androgens from being converted into estrogen, and they are frequently used to treat breast cancers that express the estrogen receptor. Unfortunately, some patients' tumors never respond to these drugs, and others gradually become resistant over time. Although the development of resistance to aromatase inhibitors has been investigated in some previous studies and some potential mechanisms have been proposed, much about this process remains unknown.

Pathiraja and colleagues began by performing a genome-wide methylation screen in breast cancer cells, which identified the developmental gene *HOXC10* as a target of epigenetic silencing in the context of long-term estrogen withdrawal. When *HOXC10* is active, it interferes with proliferation and can stimulate apoptosis, but estrogen suppresses its activity, thereby promoting tumor growth. By decreasing estrogen production, aromatase inhibitors up-regulate *HOXC10*, accounting for some of their antitumor activity. However, long-term estrogen deprivation eventually has the opposite effect, leading to methylation of *HOXC10* and its long-term suppression even in the absence of estrogen. These findings suggest that a rational approach for overcoming aromatase resistance in breast cancer may involve the addition of demethylating drugs to overcome the methylation of *HOXC10* and take advantage of its antitumor effects, although this remains to be demonstrated directly.

Science Translational Medicine (print ISSN 1946-6234; online ISSN 1946-6242) is published weekly, except the last week in December, by the American Association for the Advancement of Science, 1200 New York Avenue NW, Washington, DC 20005.

CANCER

Epigenetic Reprogramming of *HOXC10* in Endocrine-Resistant Breast Cancer

Thushangi N. Pathiraja,[1,2]* Shweta R. Nayak,[3] Yuanxin Xi,[4] Shiming Jiang,[2†] Jason P. Garee,[2‡] Dean P. Edwards,[4,5] Adrian V. Lee,[2,6] Jian Chen,[6] Martin J. Shea,[2] Richard J. Santen,[7] Frank Gannon,[8§] Sara Kangaspeska,[8¶] Jaroslav Jelinek,[9] Jean-Pierre J. Issa,[9] Jennifer K. Richer,[10] Anthony Elias,[10] Marie McIlroy,[11] Leonie S. Young,[11] Nancy E. Davidson,[6] Rachel Schiff,[2] Wei Li,[4] Steffi Oesterreich[2,6]||

Resistance to aromatase inhibitors (AIs) is a major clinical problem in the treatment of estrogen receptor (ER)–positive breast cancer. In two breast cancer cell line models of AI resistance, we identified widespread DNA hyper- and hypomethylation, with enrichment for promoter hypermethylation of developmental genes. For the homeobox gene *HOXC10*, methylation occurred in a CpG shore, which overlapped with a functional ER binding site, causing repression of *HOXC10* expression. Although short-term blockade of ER signaling caused relief of *HOXC10* repression in both cell lines and breast tumors, it also resulted in concurrent recruitment of EZH2 and increased H3K27me3, ultimately transitioning to increased DNA methylation and silencing of *HOXC10*. Reduced *HOXC10* in vitro and in xenografts resulted in decreased apoptosis and caused antiestrogen resistance. Supporting this, we used paired primary and metastatic breast cancer specimens to show that *HOXC10* was reduced in tumors that recurred during AI treatment. We propose a model in which estrogen represses apoptotic and growth-inhibitory genes such as *HOXC10*, contributing to tumor survival, whereas AIs induce these genes to cause apoptosis and therapeutic benefit, but long-term AI treatment results in permanent repression of these genes via methylation and confers resistance. Therapies aimed at inhibiting AI-induced histone and DNA methylation may be beneficial in blocking or delaying AI resistance.

INTRODUCTION

About 70% of breast tumors express estrogen receptor α (ER), and patients with these tumors are candidates for endocrine therapy such as tamoxifen and aromatase inhibitors (AIs). Despite the well-documented benefits of endocrine therapy, not all patients with ER^+ tumors initially respond to endocrine therapy ("de novo resistance"), and many ER^+ tumors eventually become refractory to therapy ("acquired resistance") (*1*). AIs, which block the conversion of androgen to estrogen and thus lower systemic estrogen, have superior efficacy for the treatment of postmenopausal ER^+ breast cancer compared to tamoxifen (*2*). Although a large body of literature has identified possible mechanisms of resistance to tamoxifen, little is known about the mechanisms of resistance to AIs (*3*).

A number of possible mechanisms for endocrine resistance have been described, such as the bidirectional crosstalk between steroid receptors and growth factor receptors (*4*). The targeting of mTORC1 (mammalian target of rapamycin complex 1) with everolimus has recently shown great promise in the treatment of endocrine-resistant ER^+ disease (*5*). Deregulation of estrogen signaling and altered expression of coactivators and corepressors have been reported to be associated with endocrine resistance (*6*). This occurs as a consequence of genetic changes, such as amplification of AIB1 (*7*), ERBB2 (*8*), and, more recently, ESR1 mutations (*9*). However, there is increasing evidence implicating epigenetic mechanisms in the development of resistance. For example, resistance to tamoxifen has been associated with promoter hypermethylation and hypomethylation of a number of genes (*10*). In contrast, very few studies have focused on epigenetic changes in breast cancer cells resistant to estrogen deprivation (*11*).

We performed a genome-wide methylation screen using two independent long-term estrogen-deprived cell lines derived from MCF-7, termed C4-12 and LTED. We identified genome-wide hyper- and hypomethylation with enrichment for developmental genes, including a number of homeobox genes. *HOXC10*, a gene repressed by estrogen in hormone-responsive MCF-7 cells, was repressed through epigenetic mechanisms after estrogen withdrawal. This epigenetic reprogramming included EZH2 recruitment, repressive histone marks, and subsequent DNA methylation. We propose a model whereby estrogen represses *HOXC10* to promote tumor growth, whereas AI blocks estrogen action to induce *HOXC10*. *HOXC10* apoptotic and growth-inhibitory functions may contribute to the therapeutic effect of AI;

[1]Graduate Program in Translational Biology and Molecular Medicine, Baylor College of Medicine, Houston, TX 77030, USA. [2]Lester and Sue Smith Breast Center, Baylor College of Medicine, Houston, TX 77030, USA. [3]Center for Reproductive Endocrinology and Infertility, Magee-Womens Hospital, Pittsburgh, PA 15213, USA. [4]Dan L. Duncan Cancer Center, Baylor College of Medicine, Houston, TX 77030, USA. [5]Departments of Molecular and Cellular Biology, and Pathology and Immunology, Baylor College of Medicine, Houston, TX 77030, USA. [6]Women's Cancer Research Center, University of Pittsburgh Cancer Institute and Magee-Womens Research Institute, University of Pittsburgh Cancer Center, Department of Pharmacology and Chemical Biology, Pittsburgh, PA 15213, USA. [7]University of Virginia Health Sciences Center, Charlottesville, VA 22903, USA. [8]European Molecular Biology Laboratory, 69117 Heidelberg, Germany. [9]Fels Institute, Temple University, Philadelphia, PA 19140, USA. [10]Departments of Pathology and Medicine, University of Colorado Anschutz Medical Campus, Denver, CO 80202, USA. [11]Royal College of Surgeons of Ireland, Dublin 2, Ireland.
*Present address: Genome Institute of Singapore, Singapore 138672, Singapore.
†Present address: University of Texas MD Anderson Cancer Center, Houston, TX 77030, USA.
‡Present address: Georgetown University, Washington, DC 20057, USA.
§Present address: QIMR Berghofer Medical Research Institute, Brisbane, Queensland 4006, Australia.
¶Present address: Institute for Molecular Medicine, Helsinki 00290, Finland.
||Corresponding author. E-mail: oesterreichs@upmc.edu

however, long-term estrogen deprivation leads to permanent epigenetic silencing of *HOXC10*, which counteracts the AI-mediated induction of these genes and contributes to acquired endocrine resistance.

RESULTS

DNA methylation frequently changes in breast cancer cells resistant to estrogen deprivation

C4-12 and LTED cells, two previously established MCF-7 sublines that are resistant to estrogen deprivation, were used for the studies (Fig. 1A). C4-12 cells were previously shown to be ER^- (*12*), whereas LTED cells maintain high levels of ER (*13*). Loss of ER in C4-12 was only partially due to methylation, because the ESR1 promoter was largely unmethylated (fig. S1A). These two cell line models are representative of clinical AI-resistant breast tumors, which can be ER^+ or ER^-. They are resistant to estrogen deprivation; however, they have not undergone complete epithelial-to-mesenchymal transition (EMT), because expression of classical EMT markers (*14*) showed inconsistent changes (fig. S1B).

We performed a genome-wide methylation screen with a previously described assay (*15*), which uses affinity-based enrichment of methylated regions of DNA via a methylation binding domain (MBD). We detected a total of 267 and 301 hypermethylated genes in C4-12 and LTED, respectively, compared to MCF-7 (table S1) (fold change cutoff >2). Hypomethylation was less frequently observed, with 82 and 97 hypomethylated genes in C4-12 and LTED, respectively. There was a highly significant overlap of hypermethylated ($P = 6.1 \times 10^{-79}$) and hypomethylated genes ($P = 2.4 \times 10^{-23}$) between C4-12 and LTED (Fig. 1B), suggesting that there were many epigenetic modifications shared between these two independent models of resistance to estrogen deprivation.

Given the well-known effect of hypermethylation on gene silencing, we focused on hypermethylation events. DNA methylation peaks from the MBD-PD (pull-down) assay showed that the promoters of DOK5, BMP4, and ZFP37 were hypermethylated in C4-12 and LTED by ~5- to ~10-fold (Fig. 1C, left panel). For all three genes, bisulfite sequencing confirmed the MBD-PD result, although the actual magnitude of methylation was somewhat variable (Fig. 1C).

Seventy-two genes were commonly hypermethylated between C4-12 and LTED cells (Fig. 1B). Gene Ontology (GO) analysis showed a marked enrichment of genes involved in developmental processes (table S2). Given the increasingly recognized importance of HOX genes in tumorigenesis, we focused our subsequent studies on *HOXC10*, which was highly methylated in both C4-12 and LTED cells.

Methylation of the *HOXC10* promoter is associated with transcriptional silencing

The *HOXC10* gene has a clearly defined CpG island spanning its proximal promoter and extending over the first exon (Fig. 2A). The distal promoter region showed almost complete DNA methylation in both C4-12 and LTED, with no detectable methylation in MCF-7 (Fig. 2B). This methylated region falls into the category of "CpG island shore" methylation, an event that has been described for other cancer cells, as well as for stem cells (*16*, *17*). There was also an increase in methylation

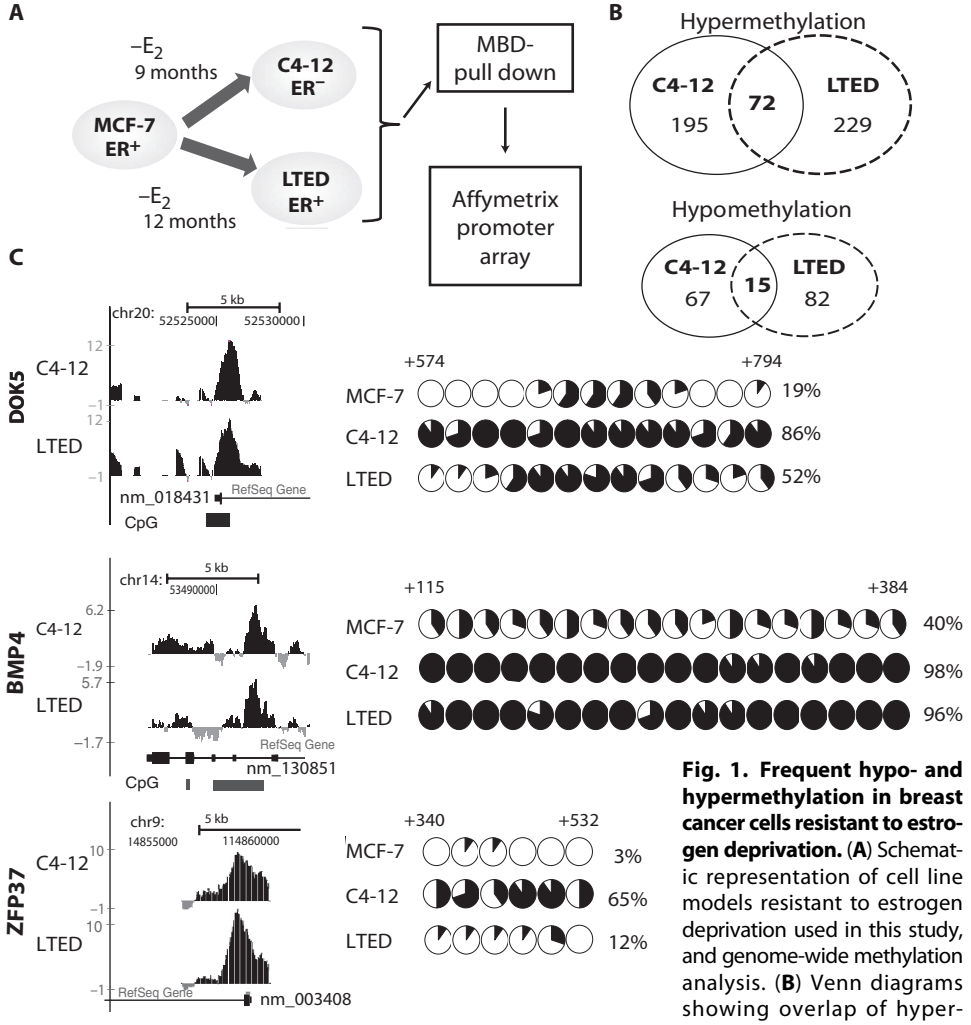

Fig. 1. Frequent hypo- and hypermethylation in breast cancer cells resistant to estrogen deprivation. (**A**) Schematic representation of cell line models resistant to estrogen deprivation used in this study, and genome-wide methylation analysis. (**B**) Venn diagrams showing overlap of hyper- and hypomethylated genes in C4-12 (solid line) and LTED (dashed line). (**C**) Confirmation of candidate hypermethylated genes identified by MBD-PD array. Methylation tracks for C4-12 and LTED compared to MCF-7 viewed on the UCSC (University of California, Santa Cruz) Genome Browser (http://www.genome.ucsc.edu/) (hg18) (left). The National Center for Biotechnology Information reference sequence IDs are indicated in the tracks. The *y* axis represents fold methylation relative to MCF-7, and upward and downward peaks represent hyper- and hypomethylated regions, respectively. Corresponding results of the bisulfite sequencing assay in MCF-7, C4-12, and LTED cells are shown on the right. Each CpG site is represented by a circle, and mean percent methylation at each CpG site is shown by the fraction of dark shading inside.

of the exonic region, although the difference between MCF-7 and the resistant cell lines was less marked. In contrast, the proximal promoter was unmethylated in MCF-7, C4-12, and LTED cells.

Quantification of *HOXC10* mRNA in MCF-7, C4-12, and LTED cells showed that methylation was associated with transcriptional silencing (Fig. 2C, top panel, and table S3). The decreased expression of *HOXC10* in breast cancer cells resistant to estrogen deprivation was not unique to MCF-7, because it was also observed in resistant cell line models generated from MDA-MB-361, ZR-75B, T47D, and BT474 breast cancer cells (Fig. 2C, bottom panel, and table S3). Treatment of C4-12, LTED, and MCF-7 cells with the DNA methylation inhibitor 5′-aza-deoxycytidine (DAC) and the histone deacetylase inhibitor trichostatin A (TSA) showed that repression of *HOXC10* was not only mediated by DNA methylation but may also involve additional repressive histone modifications (Fig. 2D and table S3). Treatment with TSA significantly induced *HOXC10* expression in both C4-12 ($P = 0.025$) and LTED cells ($P = 0.0007$), but not in MCF-7 cells ($P = 0.279$).

We analyzed *HOXC10* expression and methylation in a large number of breast cancer cell lines. Methylation at the CpG island shore varied widely from 5 to 95%, whereas very little methylation was detected at the proximal promoter region (Fig. 2E and table S3). *HOXC10* methylation at the CpG island shore and the amount of transcript were

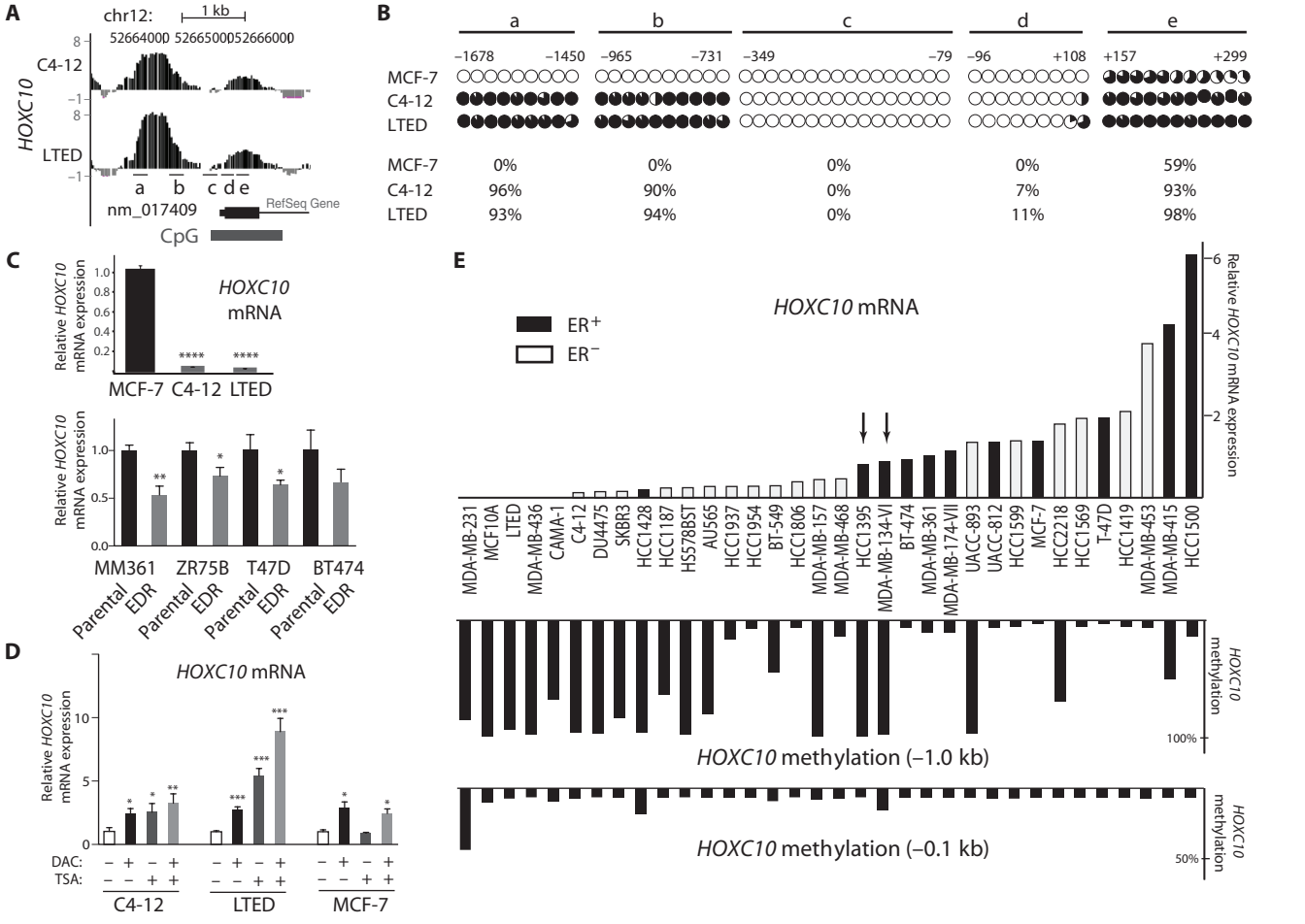

Fig. 2. Methylation and expression of *HOXC10* in breast cancer cells. (**A**) UCSC Genome Browser figure showing hypermethylated *HOXC10* regions in C4-12 and LTED cells. Methylation tracks are shown as described in Fig. 1C. The locations of bisulfite sequencing primers are depicted as lines labeled a, b, c, d, and e. (**B**) Bisulfite sequencing at an upstream promoter region/CpG shore (a and b), proximal promoter (c and d), and first exon (e) in *HOXC10*. Each CpG site is represented by a circle, and mean percent methylation at each CpG site is shown by the fraction of dark shading. (**C**) Relative mRNA expression of *HOXC10* in cells resistant to estrogen deprivation. Relative amount of mRNA is depicted as fold change compared to MCF-7 (top panel) (mean ± SD). *HOXC10* mRNA levels were determined in other ER$^+$ parental cell lines and clones resistant to estrogen deprivation ("EDR") (bottom panel). *$P < 0.05$, **$P < 0.01$ (*t* test compared to respective parental cells). Exact *P* values are provided in table S4. (**D**) Effect of DAC and TSA treatment on *HOXC10* expression. Quantitative reverse transcription polymerase chain reaction (qRT-PCR) was used to determine the relative *HOXC10* mRNA expression after C4-12, LTED, and MCF-7 cells were treated with DAC for 6 days and TSA for 14 hours. Data are means ± SD from three biological replicates and presented as fold over vehicle control. *$P < 0.05$, **$P < 0.01$, ***$P < 0.001$ (*t* test compared to vehicle-treated cells). Exact *P* values are provided in table S4. (**E**) *HOXC10* methylation inversely correlates with gene expression in breast cancer cell lines. qRT-PCR and bisulfite pyrosequencing were used to quantify expression of *HOXC10* and promoter methylation, respectively, in 34 breast cancer cell lines. ER status of the cell lines is shown by black (ER$^+$) and white (ER$^-$) boxes. The relative mRNA level is depicted as fold change compared to the average set as 1. Exact *P* values (Spearman rank correlation comparing expression and methylation) are provided in table S4.

inversely correlated ($r = -0.61$, $P = 0.001$), with a weaker association at the proximal promoter region ($r = -0.36$, $P = 0.034$). There was also an association between *HOXC10* mRNA expression and ER status of the cell lines: most ER^+ cell lines (76%) expressed *HOXC10* above the average level, but only 28% of ER^- cell lines expressed *HOXC10* above the average level. Intriguingly, the two ER^+ cell lines in which *HOXC10* was hypermethylated (MDA-MB-134-VI and HCC1395, indicated with arrows in Fig. 2E) showed decreased estrogen response compared to other ER^+ cells (fig. S2), suggesting that there is an inverse correlation between *HOXC10* methylation and ER level and function.

Estrogen regulates HOXC10 expression

The preferential expression of *HOXC10* in ER^+ cells (Fig. 2E) indicated that regulation of *HOXC10* expression might be under estrogen control. The *HOXC10* promoter has six half estrogen response element (ERE) sites and one palindromic full ERE site, with only one mismatch compared to the consensus ERE (Fig. 3A). The ERE maps to the CpG island shore, which is hypermethylated in the C4-12 and LTED cells, as well as in many ER^- cell lines. Chromatin immunoprecipitation (ChIP) assays revealed strong estrogen-induced ER recruitment to the ERE at the −1.6-kb region and modest recruitment to the −0.1-kb region (Fig. 3B

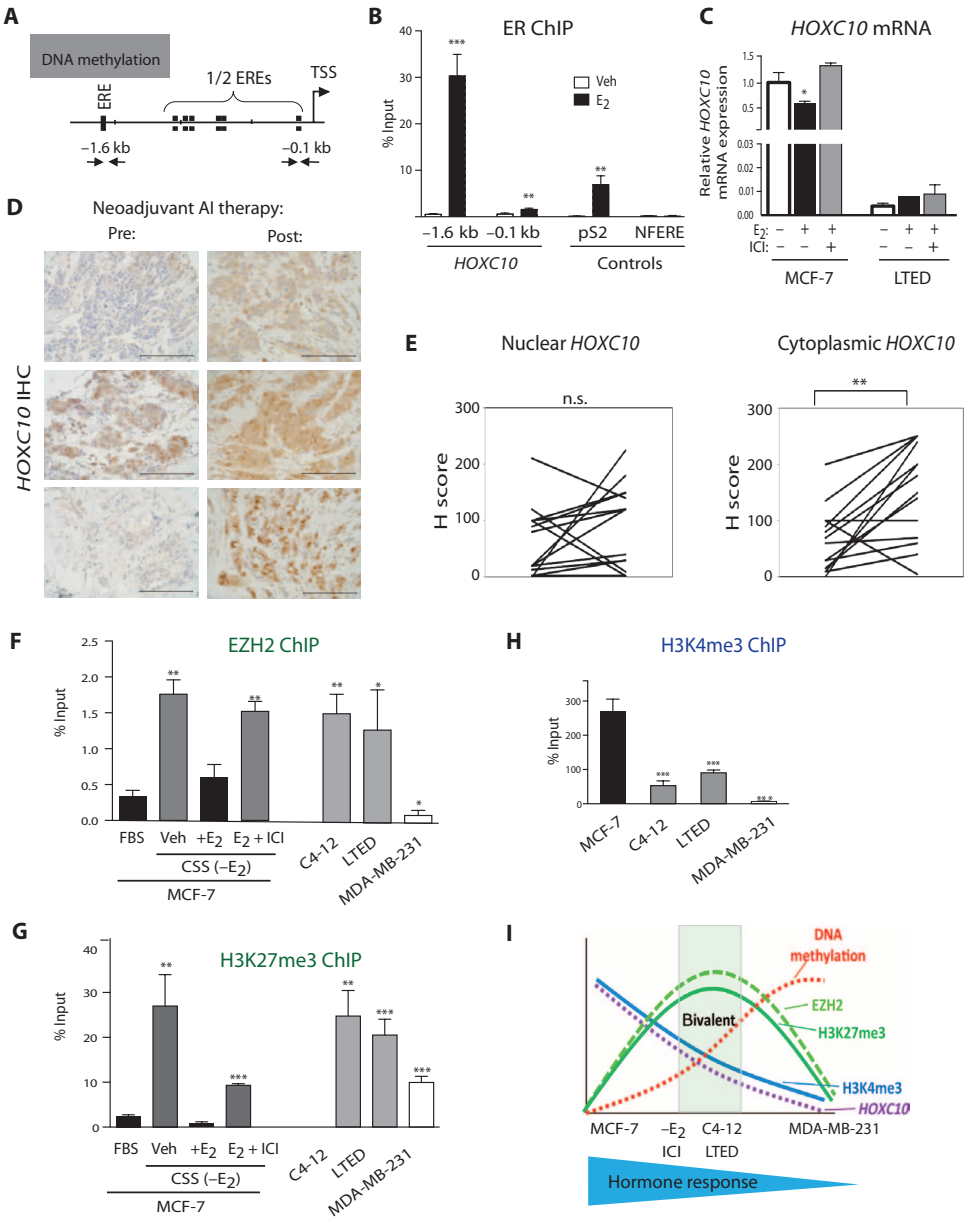

Fig. 3. Estrogen regulation of *HOXC10* expression and histone marks in the *HOXC10* promoter. (**A**) Model showing ERE sites in the *HOXC10* promoter and the position of the primers used in ChIP assays. The hypermethylated CpG shore region is shown by a shaded box. TSS, transcription start site. (**B**) ER ChIP assays in MCF-7 cells. Cells were treated with vehicle or E_2 (45 min), and ER recruitment to different positions in the *HOXC10* promoter, pS2 (positive control), and NFERE (negative control) was determined. Bars represent means ± SD from three biological replicates. $^{**}P < 0.01$, $^{***}P < 0.001$ (*t* test comparing vehicle- and E_2-treated cells). Exact *P* values are provided in table S4. (**C**) Estrogen-mediated repression of *HOXC10*. The relative mRNA expression, measured by qRT-PCR, is depicted as ligand-mediated fold change compared to vehicle (ethanol). Cells were treated for 16 hours with either vehicle, E_2, or E_2 and ICI. $P = 0.0236$ (*t* test compared to vehicle-treated cells). (**D**) *HOXC10* protein expression in clinical breast cancer specimens. Representative samples of *HOXC10* IHC in ER^+ tumors acquired before (pre) and after (post) neoadjuvant AI therapy. Scale bars, 100 μm. (**E**) Quantification of *HOXC10* protein expression in clinical breast cancer specimens. Graphical presentation of nuclear and cytoplasmic H scores. $P = 0.003$ (paired *t* test). n.s., not significant. (**F**) EZH2 recruitment at the *HOXC10* −1.6-kb site after short- and long-term E_2 deprivation. EZH2 and H3K27me3 ChIP assays in MCF-7 cells after culturing in fetal bovine serum (FBS) or in CSS (3 days) followed by treatment with vehicle, E_2, or E_2 and ICI (45 min). Bars represent means ± SD from three biological replicates. $^{*}P < 0.05$, $^{**}P < 0.01$ (left panel: *t* test compared to vehicle-treated cells; right panel: *t* test compared to MCF-7). Exact *P* values are provided in table S4. (**G**) H3K27me3 marks at the *HOXC10* −1.6-kb site after short- and long-term E_2 deprivation. Treatments in ChIP studies were performed and analyzed as in (F). $^{**}P < 0.01$, $^{***}P < 0.001$. Exact *P* values are provided in table S4. (**H**) H3K4me3 marks at the *HOXC10* −1.6-kb site. ChIP assays were performed and analyzed as in (F). $^{***}P < 0.001$. Exact *P* values are provided in table S4. (**I**) Model for associations between ER activity, *HOXC10* expression, promoter methylation, and histone marks. The central gray square ("bivalent") marks a state in which the cells have both active H3K4me3 and repressive H3K27me3.

and table S3). As a positive control, we used recruitment to pS2 ERE, and as a negative control, we used the lack of ER recruitment to a nonfunctional ERE (NFERE) (*18*). ER was also recruited (albeit more weakly) to the *HOXC10* promoter in LTED cells (fig. S3), suggesting that (i) ER can be recruited to a methylated region and (ii) ER recruitment is not sufficient for transcriptional activation.

To examine whether ER recruitment resulted in estrogen regulation of *HOXC10* gene expression, we treated MCF-7 and LTED with estradiol (E_2) and the antiestrogen ICI 182,780 (ICI). E_2 caused repression of *HOXC10* mRNA expression, which was blocked by ICI (Fig. 3C and table S3). As expected, E_2 and ICI did not change the minimal *HOXC10* expression in LTED cells. Notably, LTED cells retained the ability of estrogen to regulate many other classical E_2-regulated genes (fig. S4), consistent with a previous report (*19*). As expected, these genes were not identified in the LTED MBD-PD array as being significantly methylated, using cutoffs of $P < 10^{-5}$ and fold change of >2 in the MAT (model-based analysis of tiling arrays) analysis (table S1).

To determine whether estrogen regulation of *HOXC10* was also observed in clinical breast tumors, we measured *HOXC10* levels by immunohistochemistry (IHC) in 30 matched pre- and posttreatment samples (15 pairs) from women with early breast cancer who received 4 months of neoadjuvant exemestane treatment (Fig. 3D). Baseline expression levels varied widely; however, there was a significant increase in total *HOXC10* after short-term treatment with AI, as one would expect for an estrogen-repressed gene (paired *t* test, $P = 0.02$). This induction was more pronounced for cytoplasmic *HOXC10* ($P = 0.003$) compared to nuclear *HOXC10* (P = not significant) (Fig. 3E).

Because histone methylation is critical for long-term repression of HOX genes during embryonic development (*20*), we determined whether estrogen regulation, or loss thereof, was associated with altered EZH2 recruitment to the *HOXC10* promoter. E_2 deprivation (vehicle) of MCF-7 cells resulted in EZH2 recruitment and trimethylation of H3K27 at the distal *HOXC10* promoter region (Fig. 3, F and G, left panel, and table S3), but not at the proximal promoter (fig. S5). A similar increase in EZH2 recruitment and H3K27me3 was observed when ER signaling was blocked with ICI (Fig. 3, F and G, and table S3). A strong recruitment of EZH2 (Fig. 3F and table S3) and H3K27me3 (Fig. 3G and table S3) was also detected in C4-12 and LTED cells, with minor effects of EZH2 recruitment in the ER^- MDA-MB-231 cells, which are de novo resistant to estrogen. Because HOX genes show bivalent repressive H3K27me3 and active H3K4me marks during development (*21*, *22*), we also studied methylation at H3K4 by ChIP and found strong recruitment in MCF-7 cells, which was decreased in C4-12 and LTED and absent in MDA-MB-231 cells (Fig. 3H and table S3).

Collectively, these data suggest that short-term blockade of ER signaling is associated with increased EZH2 recruitment and increased H3K27me3, which is also seen in cells with acquired loss of hormone response (C4-12 and LTED). In these cells, chromatin is still marked by H3K4me3, thus reflecting a status of bivalent modification. DNA methylation can be observed, but it is less pronounced compared to MDA-MB-231 cells, which are fully methylated, thereby potentially decreasing the need for repressive histone modifications (depicted in a model in Fig. 3I).

Loss of *HOXC10* increases cell growth, decreases apoptosis, and enhances cell motility

To determine whether the loss of *HOXC10* is causatively involved in resistance to estrogen deprivation, we generated MCF-7 pooled clones with decreased (75 to 80%) *HOXC10* expression using two independent short hairpin RNAs (shRNAs) (Fig. 4A and table S3). MCF-7 cells with *HOXC10* knockdown (sh-H1 and sh-H2) grew significantly better ($P < 0.001$) compared to control cells with nonsilencing shRNA control (sh-ns) in the presence and absence of estrogen (Fig. 4B and table S3). This increased growth rate was associated with increased cyclin D1 levels (inset in Fig. 4B, right panel). Similar effects were observed in a second breast cancer cell line model (ZR75B). Transient knockdown of *HOXC10* in ZR75B cells resulted in increased proliferation of the cells in charcoal-stripped serum (CSS) as well as in serum-free medium (SFM), but not in full serum (Fig. 4C and table S3). This was, however, not generalizable to all resistant models, because transient knockdown of *HOXC10* had no effect in MDA-MB-361 cells and resulted in a decrease of growth in T47D cells (fig. S6). MCF-7 cells with *HOXC10* knockdown also showed increased anchorage-independent growth in the presence and absence of estrogen (Fig. 4D and table S3). We also observed increased anchorage-dependent and anchorage-independent growth of the *HOXC10* knockdown clones in the presence of tamoxifen, suggesting that *HOXC10* might have a role in tamoxifen resistance (fig. S7).

In the apoptosis analysis, we did not detect differences with E_2 in 5% CSS, but there were marked differences under estrogen-deprived conditions (Fig. 4E and table S3). In contrast to sh-ns control cells, sh-H1 cells completely lacked induction of apoptosis, and apoptosis was decreased in the sh-H2 clone. This decrease in apoptosis was reflected by a reduced induction of cleaved poly(adenosine diphosphate–ribose) polymerase (PARP) (Fig. 4E, right panel). *HOXC10* knockdown cells also displayed enhanced migration (Fig. 4, F and G, and table S3) compared to the control. In summary, loss of *HOXC10* caused MCF-7 cells to become more aggressive and less sensitive to estrogen deprivation therapy, as reflected by increased growth in two-dimensional (2D) and 3D cultures, increased motility and migration, and reduced apoptosis.

Loss of *HOXC10* promotes resistance to estrogen deprivation in vivo

To determine whether *HOXC10* plays a role in endocrine resistance in vivo, we used an endocrine resistance xenograft model. MCF-7 cells were grown in estrogen-supplemented mice, which were then randomized to receive continued estrogen supplementation or estrogen deprivation (Fig. 5A and table S3). As expected, removal of estrogen slowed growth; however, tumors soon acquired resistance to estrogen deprivation and continued to grow. Consistent with our in vitro data, *HOXC10* levels were significantly lower in the xenografts resistant to estrogen deprivation compared to the estrogen-stimulated xenografts ($P = 0.0069$) (Fig. 5B and table S3).

To directly examine the effect of *HOXC10* knockdown on endocrine sensitivity in vivo, we performed an experiment similar to Fig. 5A but injected MCF-7 control and *HOXC10* knockdown cells. In the sh-ns clone, removal of the estrogen pellet resulted in rapid shrinkage of all tumors with the exception of one outlier (Fig. 5C, left panel, and table S3). In contrast, most sh-H1 tumors continued to grow when estrogen was removed. Because the tumors in this model did not follow a homogeneous growth rate, we analyzed the tumor growth using a previously described piecewise linear ("broken stick") model (*23*) (Fig. 5C, right panel, and table S3), which clearly indicated that clone sh-H1 was resistant to estrogen deprivation. A second clone (sh-H2) grew similar to the control (fig. S8A, right panel) and did not show down-regulation of *HOXC10* levels in vivo (fig. S8B). qPCR analysis confirmed significant

down-regulation of *HOXC10* in vivo in the sh-H1 clone ($P = 0.032$) (fig. S8B). To determine whether the increased growth of the *HOXC10* sh-H1 clone in vivo was a result of decreased apoptosis and/or increased proliferation, we repeated the experiment, but tumors were harvested at an earlier time point so that the material was available for in situ analysis. As expected, estrogen removal caused a decrease in proliferation and an increase in apoptosis; however, these effects were attenuated in sh-H1 (Fig. 5D and table S3). Collectively, these data suggest that loss of *HOXC10* can confer resistance to estrogen deprivation in vivo, and the main mechanism of action is prevention of apoptosis.

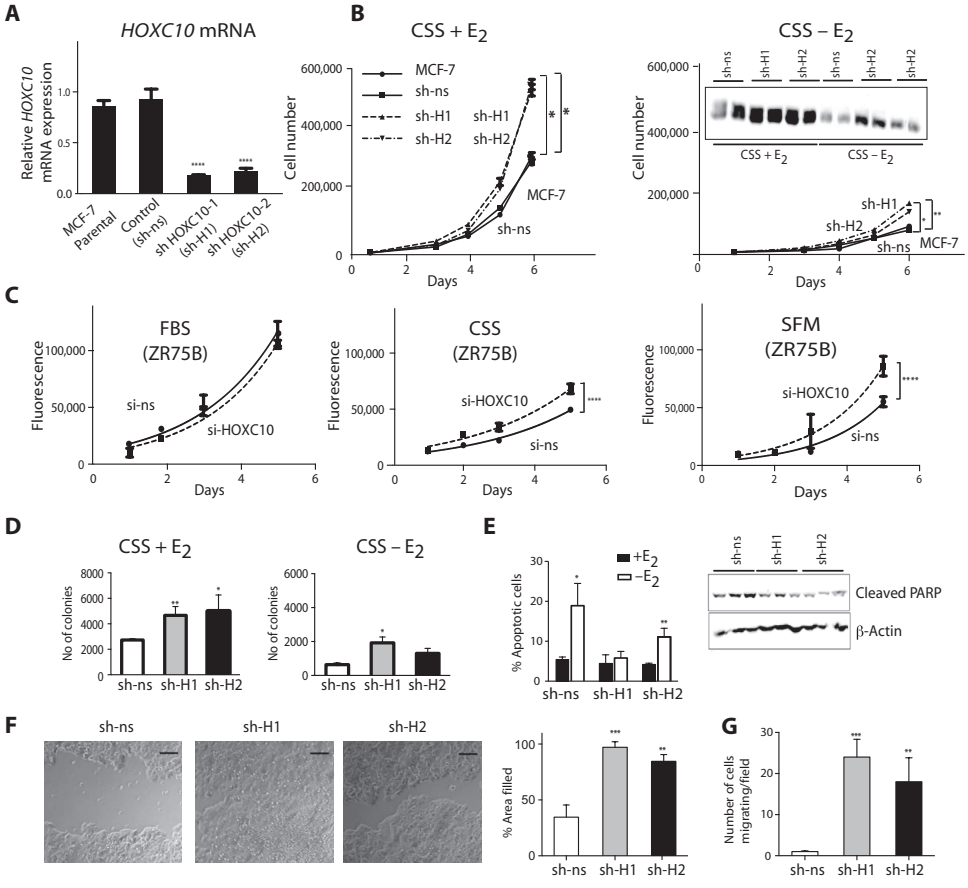

Fig. 4. Effect of *HOXC10* loss on cell growth, apoptosis, and cell motility. (**A**) shRNA-mediated knockdown of *HOXC10* expression. *HOXC10* expression was analyzed by qRT-PCR in MCF-7 parental, control (sh-ns), and *HOXC10* knockdown (sh-H1 and sh-H2) cells. Data are means ± SD from three biological replicates. ***$P < 0.001$ (*t* test compared to sh-ns). Exact *P* values are provided in table S4. (**B**) *HOXC10* knockdown increases cell proliferation. Growth curves are shown for MCF-7, sh-ns, sh-H1, and sh-H2 cells in CSS + 10^{-8} M E_2, or CSS + vehicle ($-E_2$). Data are means ± SEM from three biological replicates. *$P < 0.05$, **$P < 0.01$ (regression analysis comparing sh-H1 or sh-H2 to sh-ns). Exact *P* values are provided in table S4. The inset shows a cyclin D1 immunoblot from parallel cultures. (**C**) *HOXC10* knockdown increases proliferation in ZR75B cells. Growth curve after transient transfection with scramble small interfering RNA (siRNA) (si-ns) or with *HOXC10* siRNA and incubation in FBS, CSS, or SFM. Data are means ± SEM from seven biological replicates. ****$P <$ 0.001 (regression analysis). Exact *P* values are provided in table S4. (**D**) *HOXC10* knockdown stimulates anchorage-independent growth. sh-ns, sh-H1, and sh-H2 cells were plated in soft agar with CSS in the presence (10^{-8} M) or absence of E_2. Data are means ± SD from three biological replicates. *$P < 0.05$, **$P < 0.01$ (*t* test). Exact *P* values are provided in table S3. (**E**) shRNA-mediated knockdown of *HOXC10* reduces apoptosis. sh-ns, sh-H1, and sh-H2 cells were cultured in CSS in the presence or absence of vehicle or 10^{-8} M E_2 for 4 days, followed by measurement of apoptosis using annexin V binding assay. Data are means ± SD from three biological replicates. The right panel shows immunoblotting for cleaved PARP (and β-actin as a loading control) using the indicated lysates at 0, 3, and 6 hours after switching to CSS ($-E_2$). (**F**) shRNA-mediated knockdown of *HOXC10* enhances cell motility. sh-ns, sh-H1, and sh-H2 were seeded at the same density, scratched, and photographed 72 hours later. Scale bars, 50 μm. Data are means ± SD from three biological replicates. **$P < 0.01$, ***$P < 0.001$. Exact *P* values are provided in table S4. (**G**) shRNA-mediated knockdown of *HOXC10* enhances cell migration. Migration assays were performed in Boyden chambers with 5% serum as chemoattractant. Migrating cells were counted in three different fields, and three biological replicates were used to calculate means ± SD. **$P < 0.01$, ***$P < 0.001$. Exact *P* values are provided in table S4.

HOXC10 levels are reduced in breast tumors that recur on AI therapy

To determine whether *HOXC10* is lost in breast tumors that recur during AI therapy, we measured *HOXC10* in five matched primary-recurrent tumor pairs (Fig. 6A). We measured *HOXC10* by IHC (Fig. 6B) or qPCR (Fig. 6C), depending on the source of specimens [formalin-fixed, paraffin-embedded (FFPE) or frozen]. Supporting our hypothesis, we found decreased *HOXC10* in four of five recurrences. In the remaining pair (RCS#2), *HOXC10* was already undetectable in the primary tumor. We also measured *HOXC10* in two matched primary-recurrent tumor pairs from tamoxifen-treated patients (RCS#4 and RCS#5), and again, we detected decreased *HOXC10* expression in the recurrences (Fig. 6B). Thus, *HOXC10* levels are low in recurrences from endocrine-treated breast tumors, providing evidence for clinical relevance of our findings.

DISCUSSION

We report that *HOXC10* promoter methylation is a determinant of endocrine resistance in breast cancer. An unbiased genome-wide promoter methylation screen under long-term estrogen-deprived C4-12 and LTED cells identified widespread genomic hyper- and hypomethylation, with hypermethylation being threefold more frequent than hypomethylation. We report *HOXC10* methylation and subsequent loss of expression causing aggressive in vitro and in vivo tumor growth in the absence of estrogen, primarily mediated by loss of apoptosis. *HOXC10* expression is repressed by estrogen in vitro and in vivo to promote tumor growth. Short-term estrogen withdrawal induces *HOXC10* to induce growth arrest and apoptosis, but its long-term absence results in permanent repression

mediated by methylation. This repression counteracts the therapeutic benefit of estrogen withdrawal.

There is increasing evidence implicating HOX genes in cancer (*24*). Deregulation of HOX gene expression is frequently caused by epigenetic changes, including DNA methylation (*25*). There is also previous evidence for a role of HOX genes in endocrine treatment response in breast cancer (*26*); however, these studies were performed in the setting of tamoxifen resistance, whereas our study focuses on resistance to AI.

HOXC10 encodes a transcription factor containing a conserved DNA binding homeodomain (*27*). *HOXC10* has also been implicated in replication, where it binds in a structure-dependent manner to origins of replication and contributes to the assembly of replicative complexes (*28*, *29*). Our finding of strong regulation of *HOXC10* in the cytoplasm also implies a role for *HOXC10* outside the nucleus. Further studies will need to focus on the mechanism of action of *HOXC10* in cancer cells to understand how *HOXC10* mediates its effects on proliferation, apoptosis, and invasive phenotypes.

Intriguingly, in cervical cancer cells, *HOXC10* is associated with increased invasiveness (*30*). We also observed high *HOXC10* expression in a subset of primary tumors (as shown in our IHC studies), and knockdown of *HOXC10* decreased the growth of T47D cells and did not affect growth in MDA-MB-361. A recent study by Ansari *et al.* suggested estrogen induction of *HOXC10* (*31*). The different roles for *HOXC10* may depend on cell type and specific genetic background, an observation with increasing relevance in the era of "personalized" medicine. It is also possible that *HOXC10* might play a role in some ER^+/ER^- primary tumors that is different from its role in tumors with acquired endocrine resistance. There is an increasing realization that the mechanism involved in primary resistance might be different from those involved in secondary (acquired) resistance, with the identification of ESR1 mutations being a recent example (*9*), and it is thus critical to model these diverse clinical observations in vitro.

Finally, our studies contribute to a general model of epigenetic reprogramming in endocrine resistance. Given the estrogen regulation of HOX gene expression (*31*) and the previously reported links between ER and EZH2 (*32*), we analyzed the role of EZH2 and H3K27me3/H3K4me3 in the progression to AI resistance. In embryonic stem (ES) cells, polycomb proteins are recruited to the *HOXC10* promoter, which displays both H3K4me3 and H3K27me3 marks (*33*). These bivalent modifications frequently mark genes that are central to the developmental potential of ES cells and that are required to be in a "poised" state, ready to be transcriptionally regulated (*34*). In MCF-7 cells, the *HOXC10* regulatory region contains open chromatin marked by H3K4me3, thus allowing for

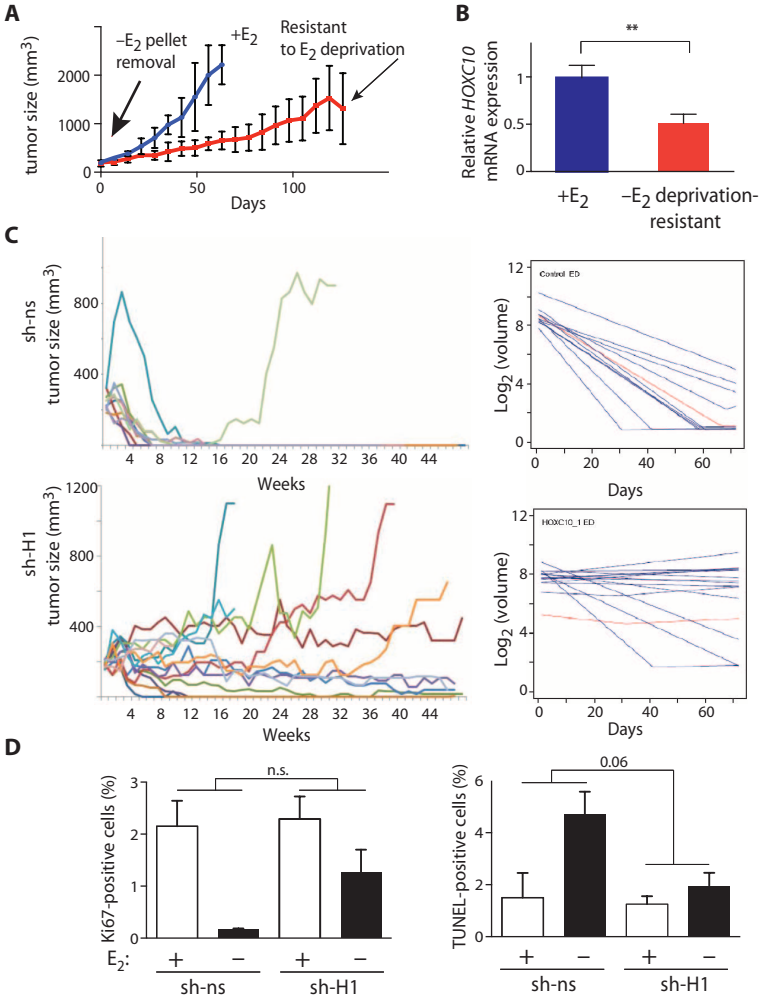

Fig. 5. Effect of *HOXC10* knockdown on endocrine resistance in breast tumor xenografts. (**A**) Growth of MCF-7 xenografts. Ovariectomized athymic nude mice bearing tumors derived from MCF-7 cells were randomly assigned to $+E_2$ (continued estrogen supplementation via E_2 pellet) or to $-E_2$ (estrogen deprivation; removal of E_2 pellet). This resulted in growth retardation, followed by outgrowth of resistant clone(s). Data are means ± SD of tumor growth from three independent mice in each group. (**B**) *HOXC10* mRNA is down-regulated in endocrine-resistant xenografts. qRT-PCR was used to quantify *HOXC10* mRNA in $+E_2$ tumors and $-E_2$-resistant tumors [from the experiment shown in (A)]. The relative mRNA expression is depicted as fold change compared to $+E_2$ group and represents means ± SD ($n = 3$ mice per group). $P = 0.0069$ (*t* test). (**C**) Down-regulation of *HOXC10* causes resistance to estrogen deprivation. sh-ns ($n = 10$) and sh-H1 ($n = 13$) cells were injected into nude mice, E_2 pellet was removed when tumors reached 150 to 200 mm^3, and tumor volume was measured over time. Right panel: Comparisons of estimated animal profiles (blue) to estimated population profile (red) for sh-ns and sh-H1 clones. For this analysis, we used the piecewise linear model for each animal's log-transformed tumor volume over time (*23*). (**D**) Increased proliferation and decreased apoptosis in *HOXC10* knockdown xenograft. Tumors from sh-ns and sh-H1 clones grown for 3 weeks in the presence or absence of E_2 were harvested and stained by IHC for Ki67 ($n = 6$ to 9) and TUNEL (terminal deoxynucleotidyl transferase–mediated deoxyuridine triphosphate nick-end labeling) ($n = 3$ to 6) to determine the effects on proliferation and apoptosis, respectively. Two-way analysis of variance (ANOVA) was used to compare effects on proliferation and apoptosis between sh-ns and sh-H1.

A

Sample ID[i]	Site of recurrence	TTR (months)	Treatment	*HOXC10* down-regulation in Met
RCS#1	Chest wall	32	AI	Yes
RCS#2	Lung	36	AI	No[iii]
RCS#3	Local	12	AI	Yes
RCS#4	Peritoneal[ii]	72	Tam	Yes
RCS#5	Cutaneous	68	Tam	Yes
05-252	Local	22	AI	Yes
06-693	Lymph nodes	17	AI	Yes

i) Samples are from RCS bank (RCS#1-5) (FFPE) and from HSTB bank (05-252; 06-693) (frozen).

ii) Pre-sacral

iii) Expression was absent in primary tumors, too.

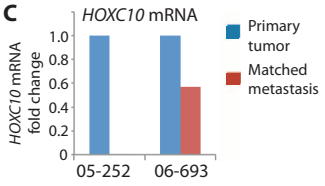

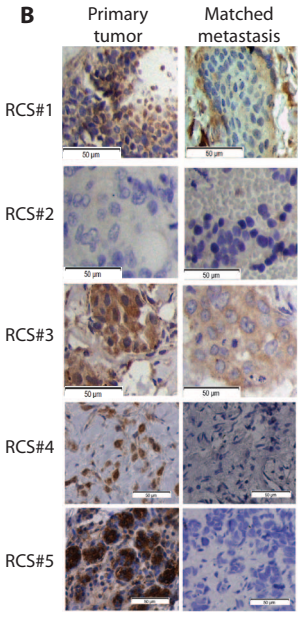

Fig. 6. *HOXC10* expression in breast tumor recurrences from AI-treated patients. (**A**) Clinical information about recurrent tumors. TTR, time to recurrence. (**B**) *HOXC10* protein expression in matched primary and recurrent tumors. FFPE samples from primary tumors and recurrences in chest wall, lung, and breast were stained for *HOXC10* by IHC. Scale bars, 50 μm. (**C**) *HOXC10* RNA expression in matched primary and recurrent tumors. *HOXC10* was measured by qPCR in primary tumors and matched recurrences, and data are presented relative to the levels in the primary tumor. $n = 1$ for each sample.

estrogen response. Loss of hormone response, such as in C4-12 and LTED cells, is associated with increased EZH2 recruitment and H3K27 trimethylation. ER and EZH2 may compete with each other for binding to the −1.6-kb region in the *HOXC10* promoter, and loss of ER signaling then results in recruitment of EZH2. In C4-12 and LTED, the *HOXC10* regulatory region contains both the H3K27me3 and H3K4me3 marks, and thus, the *HOXC10* promoter has bivalent modifications similar to ES cells, suggesting a potential "dedifferentiation." Increased H3K27me3 is accompanied by increasing hypermethylation, presumably through interaction between EZH2 and DNA methyltransferases (*35*), resulting in "epigenetic switching." Exposure of mammospheres to estrogen has been shown to promote a repressive mode of chromatin, followed by DNA methylation (*36*). Given that a number of developmental genes were methylated in our study, our results support a model of epigenetic reprogramming during transition from undifferentiated cells to hormone-responsive cells, and finally to a state characterized by hormone resistance.

Our present study has some limitations. First, the identification of methylated candidate regions was limited by the use of an Affymetrix array that contains promoters of >25,000 genes but does not contain non-promoter regions, which could be differentially methylated and important in AI resistance. Additional studies using recently developed methods, such as genome-wide bisulfite sequencing followed by systems biology analyses, will provide further insight. Second, given the relatively small sample size of the clinical specimens, it is not clear how generalizable our findings are. Additional cell lines and tumors, both primary and metastatic, representing different molecular subtypes, will need to be studied to address this limitation.

Notwithstanding these shortcomings, our study clearly provides evidence that methylation of the estrogen-regulated gene *HOXC10* is a causative event in resistance to estrogen deprivation, and it is likely that similar epigenetic reprogramming mechanisms will be observed for other developmental genes. Our data warrant additional studies to expand our understanding of epigenetic contributions to AI resistance in breast cancer and its therapeutic implications, with a specific emphasis on the early targeting of enzymes that mediate histone modifications. We expect that such interventions will be beneficial in blocking or delaying AI resistance.

MATERIALS AND METHODS

Study design

The study was designed to identify differentially methylated genes in models of AI resistance. The mechanism of repression of a candidate gene (*HOXC10*) was studied in cell line models, and the effects of loss of *HOXC10* expression were evaluated in cell lines in vitro and in vivo. Methylation, expression, cellular proliferation in 2D and 3D, apoptosis, and signaling were monitored by methylation-specific PCR, bisulfite sequencing, standard growth assays, immunoprecipitation-based approaches, histology, qPCR, immunoblotting, and IHC methods. In vitro assays were repeated two to three times. *HOXC10* expression was also studied in clinical specimens obtained from a neoadjuvant endocrine trial and from retrospective collections of matched primary and metastatic samples from breast cancer patients. Sample sizes for most studies were determined on the basis of previous knowledge or expected effect sizes, and for some analyses using clinical samples, we were restricted by the availability of the specimens. For the xenograft studies, the animals were randomly assigned to the treatment groups (−/+ estrogen and sh-ns/sh-H1/sh-H2). Full experimental details are provided below and in the Supplementary Materials.

Cell lines

Human breast cancer cell lines from the National Cancer Institute (NCI) ICBP-43 panel were cultured according to American Type Culture Collection (ATCC) instructions. C4-12 and LTED cells were maintained as previously described (*12*, *37*). Additional long-term estrogen-deprived cells were generated through incubation of cells (ZR75B, T47D, BT474, and MDA-MB-361) in CSS. Parental and estrogen-deprived MDA-MB-361 cells were provided by C. Arteaga and have previously been described (*19*). Generation of *HOXC10* knockdown clones is described in Supplementary Materials and Methods.

Glutathione *S*-transferase–MBD-PD and promoter array

Glutathione *S*-transferase–MBD-PD was performed as previously described (*15*) and as stated in Supplementary Materials and Methods.

Data were analyzed using MAT as previously described (*38*). Cutoffs used were $P < 10^{-5}$ and fold change >2.

Xenograft studies

Xenograft experiments were performed as previously published (*39*) and are detailed in Supplementary Materials and Methods. The animal experiments were performed according to protocols approved by the Institutional Animal Care and Use Committee at Baylor College of Medicine (Houston, TX).

Immunohistochemistry and immunofluorescence

To measure *HOXC10* after short-term AI treatment, tumors were obtained from a phase 2 clinical trial in which breast cancer patients were treated with exemestane alone ($n = 14$ pairs of pre- and posttreatment samples) or exemestane and tamoxifen ($n = 1$) for 4 months, as described by Harvell *et al.* (*40*). Tumor samples were obtained from pretreatment core needle biopsies and at the final excision surgery. The protocol was approved by the Colorado Multiple Institutional Review Board (COMIRB Protocol 01-627), and informed consent was obtained from all patients before participation. Studies with matched primary and metastatic samples were covered by the Ethics Committee, Beaumont Hospital, Dublin (RCS samples), and by an IRB from the University of Pittsburgh (HSTB samples).

Statistical analysis

The two-sample *t* test was used for two-group comparisons, and unless otherwise stated, treatment groups were compared to vehicle groups. All statistical tests were two-sided. Unless otherwise indicated, "*" in figures refers to $P < 0.05$, "**" to $P < 0.01$, "***" to $P < 0.001$, and "****" to $P < 0.0001$. In vitro assays were repeated three times, and plotted values represent means ± SD, unless otherwise stated. Descriptive statistics were generated with GraphPad Prism.

SUPPLEMENTARY MATERIALS

www.sciencetranslationalmedicine.org/cgi/content/full/6/229/229ra41/DC1
Materials and Methods
Fig. S1. Characterization of C4-12 and LTED cells.
Fig. S2. E_2 response in MCF-7, MDA-MB-134-VI, and HCC1395.
Fig. S3. ER ChIP for LTED cells.
Fig. S4. E_2 regulation of classical ER target genes in LTED cells.
Fig. S5. Loss of E_2 response and associated modest changes in EZH2 recruitment and trimethylation of H3K27 and H3K4 at *HOXC10* proximal promoter region.
Fig. S6. Different effects of *HOXC10* knockdown on growth in breast cancer cell lines.
Fig. S7. Tamoxifen resistance mediated by loss of *HOXC10*.
Fig. S8. In vivo growth of *HOXC10* knockdown clone sh-H2.
Table S1. Differentially methylated genes in C4-12 and LTED compared to MCF-7 (see Excel file).
Table S2. Significant GO terms for hypermethylated genes in C4-12 and LTED.
Table S3. Original data for graphs that show composite results (see Excel file).
Table S4. Exact *P* values for statistical analyses (see Excel file).
Table S5. List of qPCR primers.
Table S6. List of bisulfite sequencing primers.

REFERENCES AND NOTES

1. E. A. Musgrove, R. L. Sutherland, Biological determinants of endocrine resistance in breast cancer. *Nat. Rev. Cancer* **9**, 631–643 (2009).
2. P. E. Lønning, H. P. Eikesdal, Aromatase inhibition 2013: Clinical state of the art and questions that remain to be solved. *Endocr. Relat. Cancer* **20**, R183–R201 (2013).
3. W. R. Miller, A. A. Larionov, Understanding the mechanisms of aromatase inhibitor resistance. *Breast Cancer Res.* **14**, 201 (2012).
4. C. K. Osborne, R. Schiff, Mechanisms of endocrine resistance in breast cancer. *Annu. Rev. Med.* **62**, 233–247 (2011).
5. J. Baselga, M. Campone, M. Piccart, H. A. Burris III, H. S. Rugo, T. Sahmoud, S. Noguchi, M. Gnant, K. I. Pritchard, F. Lebrun, J. T. Beck, Y. Ito, D. Yardley, I. Deleu, A. Perez, T. Bachelot, L. Vittori, Z. Xu, P. Mukhopadhyay, D. Lebwohl, G. N. Hortobagyi, Everolimus in postmenopausal hormone-receptor–positive advanced breast cancer. *N. Engl. J. Med.* **366**, 520–529 (2012).
6. V. C. Jordan, B. W. O'Malley, Selective estrogen-receptor modulators and antihormonal resistance in breast cancer. *J. Clin. Oncol.* **25**, 5815–5824 (2007).
7. S. Bautista, H. Vallès, R. L. Walker, S. Anzick, R. Zeillinger, P. Meltzer, C. Theillet, In breast cancer, amplification of the steroid receptor coactivator gene AIB1 is correlated with estrogen and progesterone receptor positivity. *Clin. Cancer Res.* **4**, 2925–2929 (1998).
8. D. J. Slamon, G. M. Clark, S. G. Wong, W. J. Levin, A. Ullrich, W. L. McGuire, Human breast cancer: Correlation of relapse and survival with amplification of the HER-2/neu oncogene. *Science* **235**, 177–182 (1987).
9. S. Oesterreich, N. E. Davidson, The search for *ESR1* mutations in breast cancer. *Nat. Genet.* **45**, 1415–1416 (2013).
10. Y. Huang, S. Nayak, R. Jankowitz, N. E. Davidson, S. Oesterreich, Epigenetics in breast cancer: What's new? *Breast Cancer Res.* **13**, 225 (2011).
11. M. P. Jansen, T. Knijnenburg, E. A. Reijm, I. Simon, R. Kerkhoven, M. Droog, A. Velds, S. van Laere, L. Dirix, X. Alexi, J. A. Foekens, L. Wessels, S. C. Linn, E. M. Berns, W. Zwart, Hallmarks of aromatase inhibitor drug resistance revealed by epigenetic profiling in breast cancer. *Cancer Res.* **73**, 6632–6641 (2013).
12. S. Oesterreich, P. Zhang, R. L. Guler, X. Sun, E. M. Curran, W. V. Welshons, C. K. Osborne, A. V. Lee, Re-expression of estrogen receptor α in estrogen receptor α-negative MCF-7 cells restores both estrogen and insulin-like growth factor-mediated signaling and growth. *Cancer Res.* **61**, 5771–5777 (2001).
13. M. H. Jeng, M. A. Shupnik, T. P. Bender, E. H. Westin, D. Bandyopadhyay, R. Kumar, S. Masamura, R. J. Santen, Estrogen receptor expression and function in long-term estrogen-deprived human breast cancer cells. *Endocrinology* **139**, 4164–4174 (1998).
14. C. Foroni, M. Broggini, D. Generali, G. Damia, Epithelial–mesenchymal transition and breast cancer: Role, molecular mechanisms and clinical impact. *Cancer Treat. Rev.* **38**, 689–697 (2012).
15. S. Kangaspeska, B. Stride, R. Métivier, M. Polycarpou-Schwarz, D. Ibberson, R. P. Carmouche, V. Benes, F. Gannon, G. Reid, Transient cyclical methylation of promoter DNA. *Nature* **452**, 112–115 (2008).
16. S. M. Pollard, S. H. Stricker, S. Beck, Preview. A shore sign of reprogramming. *Cell Stem Cell* **5**, 571–572 (2009).
17. R. A. Irizarry, C. Ladd-Acosta, B. Wen, Z. Wu, C. Montano, P. Onyango, H. Cui, K. Gabo, M. Rongione, M. Webster, H. Ji, J. B. Potash, S. Sabunciyan, A. P. Feinberg, The human colon cancer methylome shows similar hypo- and hypermethylation at conserved tissue-specific CpG island shores. *Nat. Genet.* **41**, 178–186 (2009).
18. S. A. Krum, G. A. Miranda-Carboni, M. Lupien, J. Eeckhoute, J. S. Carroll, M. Brown, Unique ERα cistromes control cell type-specific gene regulation. *Mol. Endocrinol.* **22**, 2393–2406 (2008).
19. T. W. Miller, J. M. Balko, E. M. Fox, Z. Ghazoui, A. Dunbier, H. Anderson, M. Dowsett, A. Jiang, R. A. Smith, S. M. Maira, H. C. Manning, A. M. Gonzalez-Angulo, G. B. Mills, C. Higham, S. Chanthaphaychith, M. G. Kuba, W. R. Miller, Y. Shyr, C. L. Arteaga, ERα-dependent E2F transcription can mediate resistance to estrogen deprivation in human breast cancer. *Cancer Discov.* **1**, 338–351 (2011).
20. S. Rea, F. Eisenhaber, D. O'Carroll, B. D. Strahl, Z. W. Sun, M. Schmid, S. Opravil, K. Mechtler, C. P. Ponting, C. D. Allis, T. Jenuwein, Regulation of chromatin structure by site-specific histone H3 methyltransferases. *Nature* **406**, 593–599 (2000).
21. S. P. Atkinson, C. M. Koch, G. K. Clelland, S. Willcox, J. C. Fowler, R. Stewart, M. Lako, I. Dunham, L. Armstrong, Epigenetic marking prepares the human HOXA cluster for activation during differentiation of pluripotent cells. *Stem Cells* **26**, 1174–1185 (2008).
22. B. E. Bernstein, T. S. Mikkelsen, X. Xie, M. Kamal, D. J. Huebert, J. Cuff, B. Fry, A. Meissner, M. Wernig, K. Plath, R. Jaenisch, A. Wagschal, R. Feil, S. L. Schreiber, E. S. Lander, A bivalent chromatin structure marks key developmental genes in embryonic stem cells. *Cell* **125**, 315–326 (2006).
23. L. Zhao, M. A. Morgan, L. A. Parsels, J. Maybaum, T. S. Lawrence, D. Normolle, Bayesian hierarchical changepoint methods in modeling the tumor growth profiles in xenograft experiments. *Clin. Cancer Res.* **17**, 1057–1064 (2011).
24. C. Abate-Shen, Deregulated homeobox gene expression in cancer: Cause or consequence? *Nat. Rev. Cancer* **2**, 777–785 (2002).
25. M. J. Fackler, C. B. Umbricht, D. Williams, P. Argani, L. A. Cruz, V. F. Merino, W. W. Teo, Z. Zhang, P. Huang, K. Visvananthan, J. Marks, S. Ethier, J. W. Gray, A. C. Wolff, L. M. Cope, S. Sukumar, Genome-wide methylation analysis identifies genes specific to breast cancer hormone receptor status and risk of recurrence. *Cancer Res.* **71**, 6195–6207 (2011).
26. N. Shah, K. Jin, L. A. Cruz, S. Park, H. Sadik, S. Cho, C. P. Goswami, H. Nakshatri, R. Gupta, H. Y. Chang, Z. Zhang, A. Cimino-Mathews, L. Cope, C. Umbricht, S. Sukumar, HOXB13 mediates tamoxifen

resistance and invasiveness in human breast cancer by suppressing ERα and inducing IL-6 expression. *Cancer Res.* **73**, 5449–5458 (2013).
27. N. Shah, S. Sukumar, The Hox genes and their roles in oncogenesis. *Nat. Rev. Cancer* **10**, 361–371 (2010).
28. A. Falaschi, G. Abdurashidova, G. Biamonti, DNA replication, development and cancer: A homeotic connection? *Crit. Rev. Biochem. Mol. Biol.* **45**, 14–22 (2010).
29. L. Marchetti, L. Comelli, B. D'Innocenzo, L. Puzzi, S. Luin, D. Arosio, M. Calvello, R. Mendoza-Maldonado, F. Peverali, F. Trovato, S. Riva, G. Biamonti, G. Abdurashidova, F. Beltram, A. Falaschi, Homeotic proteins participate in the function of human-DNA replication origins. *Nucleic Acids Res.* **38**, 8105–8119 (2010).
30. Y. Zhai, R. Kuick, B. Nan, I. Ota, S. J. Weiss, C. L. Trimble, E. R. Fearon, K. R. Cho, Gene expression analysis of preinvasive and invasive cervical squamous cell carcinomas identifies *HOXC10* as a key mediator of invasion. *Cancer Res.* **67**, 10163–10172 (2007).
31. K. I. Ansari, I. Hussain, S. Kasiri, S. S. Mandal, *HOXC10* is overexpressed in breast cancer and transcriptionally regulated by estrogen via involvement of histone methylases MLL3 and MLL4. *J. Mol. Endocrinol.* **48**, 61–75 (2012).
32. B. Shi, J. Liang, X. Yang, Y. Wang, Y. Zhao, H. Wu, L. Sun, Y. Zhang, Y. Chen, R. Li, Y. Zhang, M. Hong, Y. Shang, Integration of estrogen and Wnt signaling circuits by the polycomb group protein EZH2 in breast cancer cells. *Mol. Cell. Biol.* **27**, 5105–5119 (2007).
33. N. L. Vastenhouw, A. F. Schier, Bivalent histone modifications in early embryogenesis. *Curr. Opin. Cell Biol.* **24**, 374–386 (2012).
34. G. Pan, S. Tian, J. Nie, C. Yang, V. Ruotti, H. Wei, G. A. Jonsdottir, R. Stewart, J. A. Thomson, Whole-genome analysis of histone H3 lysine 4 and lysine 27 methylation in human embryonic stem cells. *Cell Stem Cell* **1**, 299–312 (2007).
35. E. Viré, C. Brenner, R. Deplus, L. Blanchon, M. Fraga, C. Didelot, L. Morey, A. Van Eynde, D. Bernard, J. M. Vanderwinden, M. Bollen, M. Esteller, L. Di Croce, Y. de Launoit, F. Fuks, The Polycomb group protein EZH2 directly controls DNA methylation. *Nature* **439**, 871–874 (2006).
36. A. S. Cheng, A. C. Culhane, M. W. Chan, C. R. Venkataramu, M. Ehrich, A. Nasir, B. A. Rodriguez, J. Liu, P. S. Yan, J. Quackenbush, K. P. Nephew, T. J. Yeatman, T. H. Huang, Epithelial progeny of estrogen-exposed breast progenitor cells display a cancer-like methylome. *Cancer Res.* **68**, 1786–1796 (2008).
37. W. Yue, J. P. Wang, M. Conaway, S. Masamura, Y. Li, R. J. Santen, Activation of the MAPK pathway enhances sensitivity of MCF-7 breast cancer cells to the mitogenic effect of estradiol. *Endocrinology* **143**, 3221–3229 (2002).
38. W. E. Johnson, W. Li, C. A. Meyer, R. Gottardo, J. S. Carroll, M. Brown, X. S. Liu, Model-based analysis of tiling-arrays for ChIP-chip. *Proc. Natl. Acad. Sci. U.S.A.* **103**, 12457–12462 (2006).
39. S. Massarweh, C. K. Osborne, S. Jiang, A. E. Wakeling, M. Rimawi, S. K. Mohsin, S. Hilsenbeck, R. Schiff, Mechanisms of tumor regression and resistance to estrogen deprivation and fulvestrant in a model of estrogen receptor–positive, HER-2/*neu*-positive breast cancer. *Cancer Res.* **66**, 8266–8273 (2006).
40. D. M. Harvell, N. S. Spoelstra, M. Singh, J. L. McManaman, C. Finlayson, T. Phang, S. Trapp, L. Hunter, W. W. Dye, V. F. Borges, A. Elias, K. B. Horwitz, J. K. Richer, Molecular signatures of neoadjuvant endocrine therapy for breast cancer: Characteristics of response or intrinsic resistance. *Breast Cancer Res. Treat.* **112**, 475–488 (2008).

Acknowledgments: We would like to acknowledge the valuable contributions from the F.G. laboratory (G. Reid, H. Brand, S. Denger, and S. Johnson) at the European Molecular Biology Laboratory (EMBL), especially with respect to technical details of the MBD-PD. We would also like to thank the Genomics Core at EMBL for their critical contribution to the project. Technical support was provided by the Proteomics and Flow Cytometry Cores at the Dan L. Duncan Cancer Center at Baylor College of Medicine (BCM) and the Biostatistics Core Facility at the University of Pittsburgh Cancer Institute (UPCI), especially by D. Normolle and K. Cooper. We would also like to acknowledge support from L. Malorni (BCM), E. Harrington (UPCI), and N. Spoelstra (University of Colorado) for IHC, C. Arteaga for providing cell line models of resistance to estrogen deprivation, and HSTB and TARPS (University of Pittsburgh) for providing and processing of tissue. Finally, we would like to thank J. Chang (Methodist Hospital Research Institute, Houston, TX) for her mentorship of T.N.P. throughout her thesis project, especially with respect to understanding the clinical relevance of her studies. **Funding:** This project was in part funded through an Alexander von Humboldt Foundation fellowship (to S.O.); a U.S. Department of Defense (DOD) predoctoral fellowship DOD 5W81XWH-06-1-0713 (to T.N.P.); NIH grants P30CA125123 (to R.S.), P30CA47904 (to N.E.D.), P50CA58183 (to R.S.), P01CA030195 (to S.O.), R01HG007538 (to W.L.), R01CA94118 (to A.V.L.), and R01CA097213 (to S.O.); Susan G. Komen for the Cure Foundation (PG12221410 to R.S.); the EIF/Lee Jeans Breast Cancer Research Program (to R.S.); SU2C/Breast Cancer Program (to R.S. and N.E.D.); Breast Cancer Research Foundation (to R.S., N.E.D., A.V.L., and S.O.); and Pennsylvania Department of Health (S.O. and A.V.L.). The Department specifically disclaims responsibility for any analyses, interpretations, or conclusions. **Author contributions:** T.N.P., S.R.N., S.J., J.P.G., D.P.E., A.V.L., J.C., M.J.S., R.J.S., F.G., S.K., J.J., J.-P.J.I., J.K.R., A.E., L.S.Y., N.E.D., R.S., W.L., and S.O. participated in design and/or interpretation of experiments or results and in acquisition and/or analysis of data and drafted and/or revised the manuscript. R.J.S. participated in design and/or interpretation of experiments or results and drafted and/or revised the manuscript. D.P.E. was primarily responsible for the data in Fig. 2E. A.E. was primarily responsible for the clinical trial and banking tissues. J.C. was primarily responsible for growth curve analyses. J.J., T.N.P., and S.R.N. were primarily responsible for DNA methylation analysis. S.K. was primarily responsible for the methylation pull-down concept and subsequent advice. W.L. and Y.X. were primarily responsible for bioinformatic analysis of methylation pull-down data. S.R.N. was primarily responsible for acquisition of human tumors and *HOXC10* expression analysis. J.K.R., M.M., and L.S.Y. were primarily responsible for advice on IHC and staining of human primary and metastatic tumors. M.J.S. and R.S. were primarily responsible for the in vivo xenograft work. A.V.L., J.C., M.J.S., R.J.S., F.G., S.K., J.J., J.K.R., A.E., L.S.Y., and S.O. provided administrative, technical, or supervisory support. **Competing interests:** The authors declare that they have no competing interests. **Data and materials availability:** The data from the MBD-PD array have been deposited into Gene Expression Omnibus database repository under GSE39783. There is a material transfer agreement and restriction on the NCI ICBP-43 breast cancer cell line kit. Cells and derivatives cannot be distributed to other laboratories that are not recipients of the cell line kit. These cell lines are now available for purchase from ATCC (Breast Cancer Cell Line Panel ATCC 30-4500K).

Submitted 18 December 2013
Accepted 3 March 2014
Published 26 March 2014
10.1126/scitranslmed.3008326

Citation: T. N. Pathiraja, S. R. Nayak, Y. Xi, S. Jiang, J. P. Garee, D. P. Edwards, A. V. Lee, J. Chen, M. J. Shea, R. J. Santen, F. Gannon, S. Kangaspeska, J. Jelinek, J.-P. J. Issa, J. K. Richer, A. Elias, M. McIlroy, L. S. Young, N. E. Davidson, R. Schiff, W. Li, S. Oesterreich, Epigenetic reprogramming of *HOXC10* in endocrine-resistant breast cancer. *Sci. Transl. Med.* **6**, 229ra41 (2014).